had the least significance. Thus, after removing the 2440 nm band as a component, the next combination was 1350, 1850, 2450 nm and, eventually, the combination 1410, 1910, 2450 nm was decided upon. In the case of clay, a fourth component (2460 nm) was added subsequently, as it increased both $r^2$ and adjusted-$r^2$ values.

In all cases, except $C_{org}$, PLS regression was most successful using the first derivative (10 nm intervals) of the spectral data. The Savitsky-Golay filter was also experimented with, though this did not improve upon first derivative regression results (as interpreted by $r^2$ values). As shown in Table 3.3.2, all equations are significant to $p < 0.01$ and all components to $p < 0.1$ (most are $p < 0.01$). $R^2$ values are comparable to those of previous studies (see appendix). Figure 3.3.5 show scatter plots of actual vs. predicted values generated by each soil indicator's equation.

**Table 3.3.2** Coefficients used to predict soil quality indicators from spectral data

| Indicator | $r^2$ | Adj-$r^2$ | RMSE | p | Band (λ nm) | Coefficient | p |
|---|---|---|---|---|---|---|---|
| Clay % (first deriv.) | 0.935 | 0.883 | 2.02 | 0.0036 | Intercept | 60.36 | 0.0003 |
| | | | | | 1410 | -83990 | 0.0007 |
| | | | | | 1910 | 84700 | 0.0017 |
| | | | | | 2450 | -21894 | 0.0595 |
| | | | | | 2460 | -13924 | 0.0659 |
| % $C_{org}$ (original reflectance) | 0.936 | 0.904 | 0.236 | 0.0006 | Intercept | 2.250 | 0.0165 |
| | | | | | 350 | 56.46 | 0.0025 |
| | | | | | 400 | 170.44 | 0.0011 |
| | | | | | 700 | -19.70 | 0.0023 |
| % N (first deriv.) | 0.840 | 0.760 | 0.021 | 0.0084 | Intercept | 0.428 | 0.0003 |
| | | | | | 360 | 56.46 | 0.0025 |
| | | | | | 410 | -276.11 | 0.0107 |
| | | | | | 760 | -811.68 | 0.0179 |
| Exch. K (first deriv.) | 0.983 | 0.974 | 0.048 | < 0.0001 | Intercept | 1.27 | < 0.0001 |
| | | | | | 1350 | 6452 | < 0.0001 |
| | | | | | 2420 | -1854 | 0.0001 |
| | | | | | 2430 | 1757 | 0.0001 |

*p-values indicate significance (from t-values)

Soil quality indicators were then predicted for the remaining 90 samples using each indicator's multivariate equation [i.e., from Table 3.3.2, exch. K (me/100 g soil) = $1.27 + 6452 \cdot X_{1350} - 1854 \cdot X_{2420} + 1757 \cdot X_{2430}$]; Figure 3.3.6 provides an example, using the derivative of a random soil sample's spectra to predict clay content. In four instances for clay and $C_{org}$, equations produced values outside of an indicator's prediction interval ($\alpha = 0.1$, performed in SAS) and these values were removed from the data set to prevent extrapolation (outliers for N and K are indicated as appendix). To correlate soil quality indicators with soil type, land use, and management practices, indicator values were averaged for all soil samples taken in a particular category (e.g., all soils from RU2, or all soils from fields with contour ridges). C/N ratio was calculated as $\%C_{org}$ over %N and trends are reported alongside those of the other indicators.

Trends in soil quality indicators were tested for significance using one-tailed t-tests (performed in SAS). Management practices (from georeferenced soil sample site descriptions) were also matched with ASTER pixels to observe their influence in SLA-NDVI and MSI values, and trends were tested for significance using one-tailed t-tests.

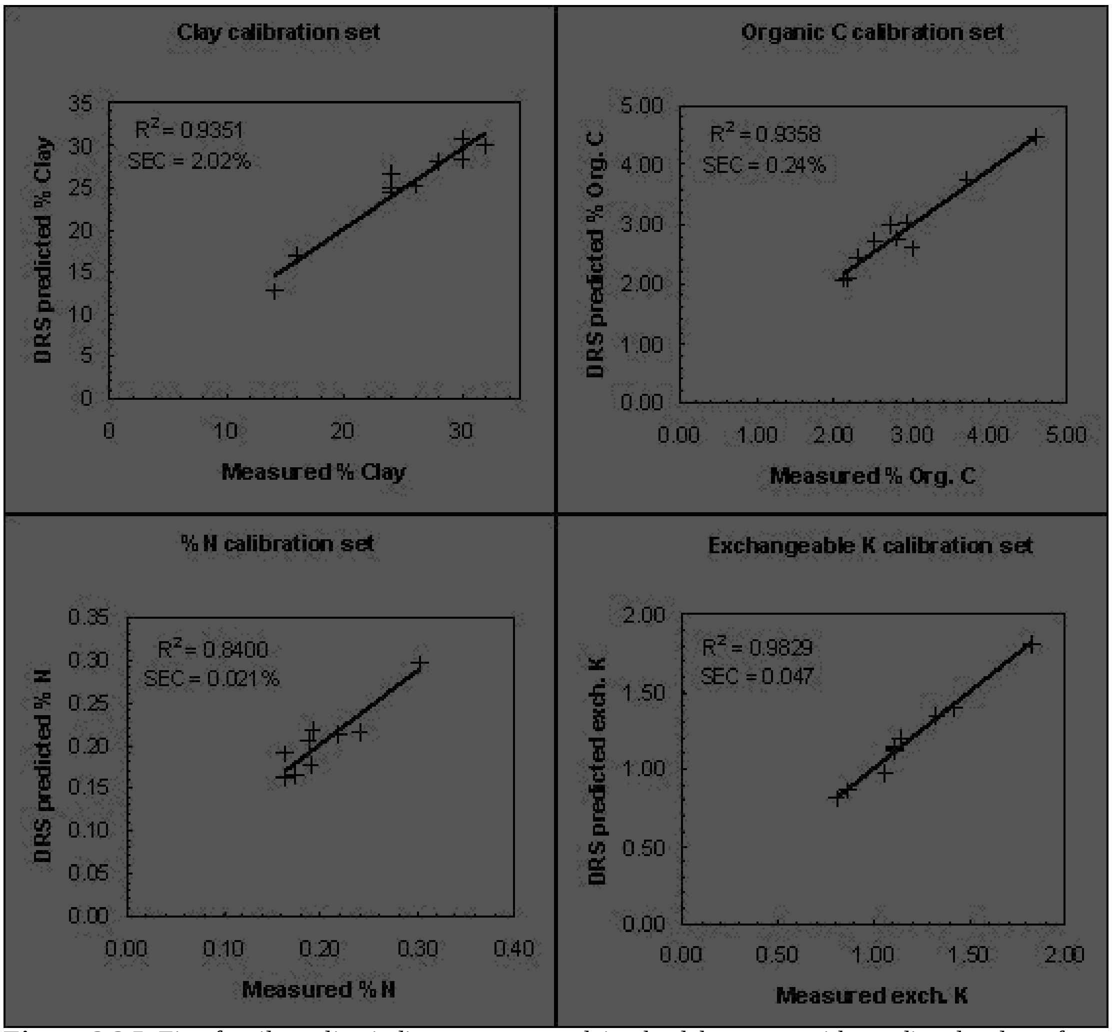


**Figure 3.3.5** Fit of soil quality indicators measured in the laboratory with predicted values from calibration to soil spectra